

CO₂ and HCO₃⁻ uptake in marine diatoms acclimated to different CO₂ concentrations

Steffen Burkhardt

Alfred Wegener Institute for Polar and Marine Research, Am Handelshafen 12, D-27570 Bremerhaven, Germany

Gabi Amoroso

Fachbereich Biologie, Universität Kaiserslautern, Postfach 3049, D-67653 Kaiserslautern, Germany

Ulf Riebesell

Alfred Wegener Institute for Polar and Marine Research, Am Handelshafen 12, D-27570 Bremerhaven, Germany

Dieter Sültemeyer¹

Fachbereich Biologie, Universität Kaiserslautern, Postfach 3049, D-67653 Kaiserslautern, Germany

Abstract

Rates of cellular uptake of CO₂ and HCO₃⁻ during steady-state photosynthesis were measured in the marine diatoms *Thalassiosira weissflogii* and *Phaeodactylum tricorutum*, acclimated to CO₂ partial pressures of 36, 180, 360, and 1,800 ppmv. In addition, in vivo activity of extracellular (eCA) and intracellular (iCA) carbonic anhydrase was determined in relation to CO₂ availability. Both species responded to diminishing CO₂ supply with an increase in eCA and iCA activity. In *P. tricorutum*, eCA activity was close to the detection limit at higher CO₂ concentrations. Simultaneous uptake of CO₂ and HCO₃⁻ was observed in both diatoms. At air-equilibrated CO₂ levels (360 ppmv), *T. weissflogii* took up CO₂ and HCO₃⁻ at approximately the same rate, whereas CO₂ uptake exceeded HCO₃⁻ uptake by a factor of two in *P. tricorutum*. In both diatoms, CO₂:HCO₃⁻ uptake ratios progressively decreased with decreasing CO₂ concentration, whereas substrate affinities of CO₂ and HCO₃⁻ uptake increased. Half-saturation concentrations were always $\leq 5 \mu\text{M}$ CO₂ for CO₂ uptake and $< 700 \mu\text{M}$ HCO₃⁻ for HCO₃⁻ uptake. Our results indicate the presence of highly efficient uptake systems for CO₂ and HCO₃⁻ in both diatoms at concentrations typically encountered in ocean surface waters and the ability to adjust uptake rates to a wide range of inorganic carbon supply.

Primary production by marine phytoplankton takes place in an environment that is characterized by high and relatively constant HCO₃⁻ concentrations (~2 mM) but low and variable concentrations of molecular dissolved CO₂ [CO_{2, aq}] (~5–25 μM). Variation in [CO_{2, aq}] of ocean surface waters is mainly caused by intense photosynthesis during phytoplankton blooms, differences in water temperature, or mixing with deep water of different CO₂ content. On longer timescales, rising CO₂ concentrations in the upper layers of the ocean are expected in response to the present increase in atmospheric CO₂ partial pressure (pCO₂; Houghton et al. 1996). Because these changes in [CO_{2, aq}] are always accompanied by changes in pH, concentrations of HCO₃⁻ vary much less because of concomitant shifts in the relative proportions of the inorganic carbon (C_i) species.

The response of phytoplankton growth to changes in CO₂ supply is largely determined by the mechanism of C_i uptake. Several studies indicate that both CO₂ and HCO₃⁻ in the bulk seawater are utilized by marine eukaryotic microalgae (e.g., Colman and Rotatore 1995; Rotatore et al. 1995; Korb et al.

1997; Tortell et al. 1997; Elzenga et al. 2000). Uptake of CO₂ may involve passive diffusion and active transport across the plasmalemma into the cell (Miller et al. 1991; Rotatore and Colman 1991, 1992; Rotatore et al. 1992, 1995; Li and Canvin 1998). Uptake of HCO₃⁻ by diffusion is restricted by the low solubility of charged molecules in membrane lipids and by the inside-negative electric potential difference across the plasmalemma in marine autotrophs (Raven 1980, 1997). Consequently, HCO₃⁻ utilization occurs either by direct active uptake or by extracellular catalytic conversion of HCO₃⁻ to CO₂ in the presence of carbonic anhydrase (CA), with CO₂ entering the cell (Badger et al. 1998; Kaplan et al. 1998; Sültemeyer et al. 1998). In the case of direct HCO₃⁻ uptake, cellular growth is expected to be more or less unaffected by external CO₂. In contrast, CA-mediated utilization of HCO₃⁻ accelerates CO₂ formation from HCO₃⁻ but has no effect on CO₂ equilibrium concentrations at the cell surface. Therefore, the presence of extracellular CA does not prevent phytoplankton from being affected by changes in extracellular [CO_{2, aq}].

The proportion at which CO₂ and HCO₃⁻ are taken up and the extent to which C_i uptake is affected by changes in CO₂ supply are still poorly quantified in marine microalgae. Evidence for HCO₃⁻ utilization is often provided by methods that do not differentiate between CA-catalyzed HCO₃⁻ use (with subsequent CO₂ uptake) and direct HCO₃⁻ uptake across the plasmalemma (e.g., Burns and Beardall 1987;

¹ Corresponding author (suelteme@rhrk.uni-kl.de).

Acknowledgments

This research was conducted as part of a German-Israeli Cooperation in Marine Science (MARS 2) under coordination of the GKSS funded by the Bundesministerium für Bildung und Forschung contract number 03F0200A.

Korb et al. 1997). Other studies infer direct HCO₃⁻ transport from pH drift experiments and the inhibition of light-dependent C_i utilization by 4'-diisothiocyanatostilbene-2,2-disulfonic acid (DIDS), which is suggested to inhibit anion exchange processes (Nimer et al. 1997). However, no quantitative estimates of C_i fluxes can be derived from this approach. Separate quantification of CO₂ and HCO₃⁻ uptake, on the other hand, is usually based on measurements under conditions at which photosynthetic carbon fluxes were not at steady state (e.g., Colman and Rotatore 1995; Rotatore et al. 1995).

The method proposed by Badger et al. (1994) provides a technique to overcome the above-mentioned shortcomings. This mass spectrometric procedure uses the chemical disequilibrium between CO₂ and HCO₃⁻ during light-dependent C_i uptake to differentiate between CO₂ and HCO₃⁻ fluxes across the plasmalemma and to quantify these fluxes during steady-state photosynthesis. Although this method has been successfully applied to different strains of the cyanobacterium *Synechococcus* (Badger et al. 1994; Sültemeyer et al. 1995, 1998), the halotolerant chlorophyte *Dunaliella tertiolecta* (Amoroso et al. 1998), and several freshwater microalgae, including isolated chloroplasts (Badger et al. 1994; Palmqvist et al. 1994; Amoroso et al. 1998), it has not yet been applied to marine diatoms that represent one of the dominant phytoplankton taxa in the ocean.

The present study was intended to estimate cellular uptake of CO₂ and HCO₃⁻ during steady-state photosynthesis in relation to external CO₂ supply in two marine diatoms by use of membrane inlet mass spectrometry. We used this approach to determine substrate preferences for CO₂ and HCO₃⁻ uptake as well as possible shifts in carbon source and C_i uptake kinetics in cells acclimated to different [CO_{2,aq}]. Furthermore, the potential role of carbonic anhydrases was evaluated in these cultures on the basis of in vivo estimates of both extracellular and intracellular CA by monitoring ¹⁸O exchange from doubly labelled ¹³C¹⁸O₂ with the same measuring system.

Material and methods

Cultures, growth conditions, and sampling—*Phaeodactylum tricornutum* (Bohlin) strain CCAP 1052/1A and *Thalassiosira weissflogii* (Grunow) Fryxell & Hasle were grown at 15°C in 0.2-μm-filtered, nutrient-enriched seawater (salinity 32) from the North Sea. Nitrate, phosphate, silicate, trace metals, ethylenediaminetetra-acetic acid (EDTA), and vitamins were added at concentrations of f/2 medium (Guillard and Ryther 1962). Batch cultures were grown in 1-liter glass tubes under continuous light at an incident photon flux density (PFD) of 120 μmol photons m⁻² s⁻¹. Different CO₂ partial pressures (pCO₂) in the medium were achieved by a continuous flow of 0.2-μm-filtered air containing 36, 180, 360, or 1,800 ppmv CO₂. Because the culture medium was not buffered artificially, an increase from 36 to 1,800 ppmv CO₂ was accompanied by a decrease in the pH from 9.1 to 7.6. Air bubbles were dispersed at the bottom of each incubation vessel through a fritted glass disk (25 mm diameter, porosity 1). Experimental cultures were acclimated to the

respective conditions for at least 48 h before harvesting. Chlorophyll *a* concentrations at the time of sampling ranged from 34 to 183 μg L⁻¹.

For measurements of CA activity or C_i uptake, 800 ml of culture were centrifuged at 3,000 × *g* and 15°C for 5 min. Subsequently, the cells were washed twice by centrifugation (3,000 × *g*, 2 min) in CO₂-free f/2 medium, buffered with 1,3-bis[tris(hydroxymethyl)methylamino]propane (BTP, 50 mM [pH 8.0], CA measurements) or 2-[4-(2-Hydroxyethyl)-1-piperazinyl]-ethanesulfonic acid (HEPES, 50 mM [pH 8.0], C_i uptake measurements). 2 × 10 μl of the resuspended pellet were used for spectrophotometric Chl *a* analysis at 652 and 665 nm after extraction in 1 ml of methanol (5 min in darkness, room temperature), followed by centrifugation (4,500 × *g*, 2 min). A subsample of 100 ml of the original culture was used for potentiometric pH measurements and cell counts. For enumeration on a Coulter multisizer, cells were preserved with Lugol's iodine.

Determination of dissolved inorganic carbon, alkalinity, [CO_{2,aq}], and [HCO₃⁻]—Cell-free subsamples of culture medium, equilibrated at the four different experimental partial pressures, were taken for measurements of total dissolved inorganic carbon (DIC) and total alkalinity (tAlk). DIC was determined coulometrically in duplicate with a system similar to that described by Johnson et al. (1993). tAlk was determined in duplicate by Gran titration with an automated, temperature-controlled system at 20°C. Concentrations of CO₂ ([CO_{2,aq}]) and HCO₃⁻ ([HCO₃⁻]) were calculated from DIC, tAlk, temperature, salinity, and concentrations of phosphate and silicate by use of the dissociation constants of Goyet and Poisson (1989).

Determination of CA activity—Activity of extracellular (eCA) and intracellular (iCA) CA was determined by measuring the loss of ¹⁸O from doubly labelled ¹³C¹⁸O₂ to water caused by several hydration and dehydration steps of CO₂ and HCO₃⁻ (Silverman 1982; Badger and Price 1989; Sültemeyer et al. 1990). Doubly labelled CO₂ was prepared from H₂¹⁸O (98 atom% enrichment) and NaH¹³CO₃ (99 atom% enrichment), both purchased from Chemotrade (Leipzig, Germany). NaH¹³CO₃ was added to H₂¹⁸O (1 M C_i final concentration) under N₂ atmosphere, sealed in an airtight glass vial, and heated at 80°C for 4 to 5 h. This procedure yielded ~80% of doubly labelled CO₂. The reaction sequence of ¹⁸O loss from ¹³C¹⁸O¹⁸O (*m/z* = 49) with the intermediate product ¹³C¹⁸O¹⁶O (*m/z* = 47), and the end product ¹³C¹⁶O¹⁶O (*m/z* = 45) was recorded in 0.5-s intervals on a quadrupole membrane inlet mass spectrometer (MSD 5970; Hewlett Packard, Waldbronn, Germany) connected to a 10-ml thermostated cuvette. Depletion of ¹⁸O in doubly labelled CO₂ is an irreversible reaction, because H₂¹⁸O produced is infinitely diluted with H₂¹⁶O.

For determination of CA activity, relative ¹⁸O enrichment was calculated from the 45, 47, and 49 signals as a function of time according to

$$\log(\text{enrichment}) = \log[49 \times 100 / (45 + 47 + 49)]. \quad (1)$$

Typical curves for *P. tricornutum* and *T. weissflogii* are shown in Fig. 1. In a first step, 10 ml of f/2 medium, buff-

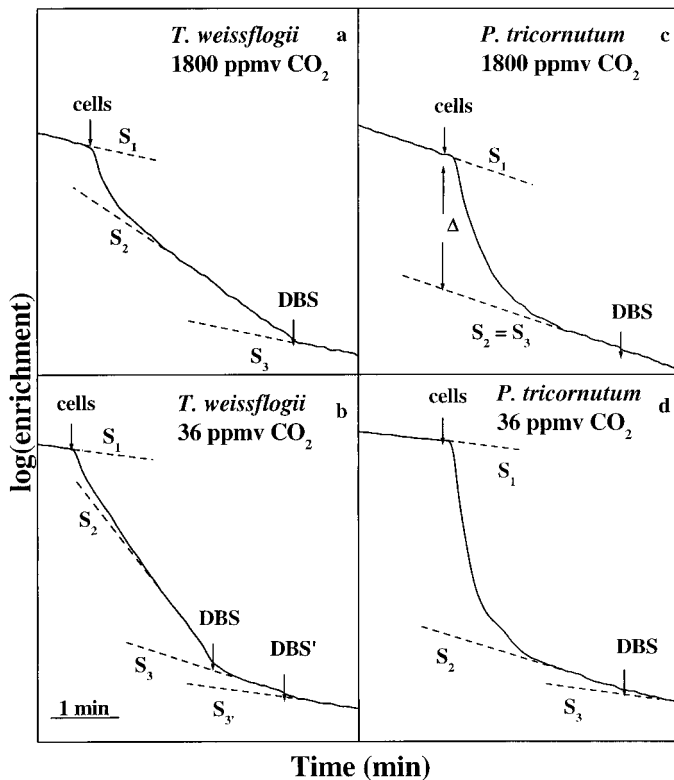


Fig. 1. In vivo measurements of CA activity based on ^{18}O exchange between doubly labelled CO_2 ($^{13}\text{C}^{18}\text{O}^{18}\text{O}$, $m/z = 49$) and water. The reaction sequence of ^{18}O loss from $m/z = 49$ to $m/z = 45$ with the intermediate product $m/z = 47$ was monitored by membrane inlet mass spectrometry and is reported as $\log(\text{enrichment})$ according to Eq. 1. The initial slope (S_1) represents ^{18}O exchange during the uncatalyzed hydration/dehydration reaction between CO_2 and HCO_3^- . The difference between S_2 and S_1 indicates ^{18}O exchange in the presence of eCA. eCA activity is calculated according to Eq. 2. S_3 and S_3' represent ^{18}O exchange upon the addition of 50 μM or 100 μM DBS (an inhibitor of eCA), respectively. The drop (Δ) in $\log(\text{enrichment})$ when S_2 is extrapolated to the time of cell addition is taken as a measure of intracellular CA activity. (a, b) Data are shown for *T. weissflogii* and (c, d) *P. tricorutum*, (a, c) acclimated to 1,800 ppmv and (b, d) 36 ppmv in nonbuffered culture medium.

ered with 50 mM BTP (pH 8.0) was injected into the cuvette and closed with a stopper for temperature equilibration (15°C). 10 μl of $\text{NaH}^{13}\text{C}^{18}\text{O}_3$ solution were added to achieve 1 mM final concentration. After chemical equilibrium was reached (initial slope, S_1), 50–100 μl of washed cells (resuspended pellet) were added to a final Chl *a* concentration of 1–3 $\mu\text{g ml}^{-1}$. To avoid interference of CO_2 measurements with light-dependent uptake of inorganic carbon by the cells, all measurements were performed in the dark. Extracellular CA activity was estimated from the enhanced rate of ^{18}O exchange, which is represented by slope S_2 in Fig. 1. Intracellular CA activity was estimated from the rapid decline in $\log(\text{enrichment})$ upon injection of cells after correction for S_2 (Palmqvist et al. 1994).

Dextran-bound sulfonamide (DBS; Synthelec AB, Lund, Sweden), an inhibitor of eCA that cannot penetrate the cell

membrane (Sültemeyer et al. 1990), was used in control measurements. DBS was added to the cuvette at various concentrations either prior to injection of doubly labelled CO_2 or during steady-state depletion of ^{18}O due to eCA activity. The resulting rates of $\log(\text{enrichment})$ in the presence of cells (slope S_3) were compared with S_2 in the absence of DBS to demonstrate that eCA was responsible for accelerated ^{18}O depletion. Furthermore, DBS concentrations were determined at which complete inhibition of eCA activity was achieved. This inhibition is a prerequisite for measurements of CO_2 uptake and HCO_3^- transport, which rely on the relatively slow spontaneous interconversion between CO_2 and HCO_3^- .

Determination of CO_2 uptake, HCO_3^- uptake, and net photosynthesis—Inorganic carbon fluxes were determined during steady-state photosynthesis by use of membrane inlet mass spectrometry. This method is described in detail by Badger et al. (1994) and has been applied in several studies since then (e.g., Palmqvist et al. 1994; Tchernov et al. 1997; Amoroso et al. 1998; Sültemeyer et al. 1998). It is based on simultaneous measurements of O_2 and CO_2 during consecutive light (4 min) and dark (3 min) intervals.

To estimate CO_2 and HCO_3^- uptake, the same membrane inlet system was used as in CA measurements. All measurements were performed at a constant pH of 8.0. Washed cells were injected into 10 ml of CO_2 -free f/2 medium, buffered with 50 mM HEPES (pH 8.0, 15°C) within 10 min after centrifugation, and the cuvette was closed immediately. Chl *a* concentrations in the cuvette were 1–3 $\mu\text{g ml}^{-1}$. DBS was added prior to cell addition at concentrations of 50–100 μM (under the assumption of 5 mol acetazolamide covalently bound to 1 mol dextran; Palmqvist et al. 1990) to assure complete inhibition of eCA activity. After 2 min of darkness and two short light periods (0.5 min each), the first light:dark cycle was initiated at 300 $\mu\text{mol photons m}^{-2} \text{ s}^{-1}$ incident PFD and a CO_2 concentration of typically $<1 \mu\text{M}$ ($C_i < 100 \mu\text{M}$). Between the subsequent light:dark cycles, known amounts of C_i were added to measure uptake rates as a function of CO_2 and HCO_3^- concentrations.

Rates of O_2 consumption in the dark and O_2 production in the light provide a direct estimate of respiration and net C_i fixation, under the assumption of a respiratory quotient of 1.0 and a photosynthetic quotient of 1.1 to convert O_2 fluxes into C_i fluxes. Gross CO_2 uptake was calculated from the steady-state rate of CO_2 depletion at the end of the light period and the initial rate of CO_2 generation immediately after the light was turned off. This calculation is based on the assumption that the rate of diffusive CO_2 efflux from a cell in the light represents the rate of CO_2 efflux during the first seconds of the dark phase.

HCO_3^- uptake was calculated from net C_i fixation, corrected for measured steady-state depletion of CO_2 at the end of the light period and for $\text{CO}_2/\text{HCO}_3^-$ interconversion in the medium. This calculation refers to net HCO_3^- uptake. As will be discussed below, gross HCO_3^- uptake equals net HCO_3^- only if diffusive efflux of HCO_3^- is negligible. In calculations, the required pseudo first-order rate constant k_2 (formation of CO_2 from HCO_3^-) was experimentally determined from the initial slope of CO_2 evolution from HCO_3^-

after injection of known amounts of HCO₃⁻ into CO₂-free buffered medium. Several independent measurements yielded a mean value (± 1 SD, $n = 10$) of $k_2 = 8.9 (\pm 1.1) \times 10^{-3} \text{ min}^{-1}$. The k_1 rate constant (formation of HCO₃⁻ from CO₂) was calculated from the product of k_2 and the ratio of CO₂ and HCO₃⁻ concentrations, which was measured daily in the freshly prepared assay medium. For further details regarding the method and calculations, we refer to Badger et al. (1994).

Effect of eCA on net photosynthesis—To investigate the potential effect of eCA on net photosynthesis, rates of photosynthetic O₂ evolution in the light were monitored in *P. tricornutum* and *T. weissflogii* in the presence and absence of eCA activity. Cultures acclimated to 36 or 180 ppmv CO₂ were used in these experiments. Changes in the O₂ concentration of the assay medium (10 ml, buffered with 50 mM HEPES [pH 8.0]) were monitored with the mass spectrometer by use of the same experimental protocol as for C_i uptake measurements. CO₂ concentrations in the medium were 1 and 13 μM . During steady-state photosynthesis in the light, DBS (100 μM final concentration) was injected into the closed cuvette to inhibit eCA activity. In additional tests, 60 μg of commercially available CA from bovine erythrocytes (Sigma Chemical Co., Munich, Germany; 4090 W-A units mg⁻¹ protein) was added during measurements of O₂ evolution in *P. tricornutum* in the absence of CA inhibitor.

Results

CA activity—As indicated in Fig. 1, CA assays yielded different curves depending on species and culture conditions. After the addition of cells, a constant rate of decrease in log(enrichment) was reached within 3–6 min. The difference between S_2 and S_1 was caused by eCA activity, as indicated by the addition of the eCA inhibitor DBS (S_3). Full inhibition of eCA was achieved upon the addition of DBS to 50 μM (Fig. 1a,d) or 100 μM (Fig. 1b) final concentration, depending on the level of activity expressed by the cells.

As a measure of eCA activity, we defined one unit as 100% stimulation of the noncatalyzed ¹⁸O depletion from ¹³C¹⁸O₂ according to the method of Badger and Price (1989):

$$U = (S_2 - S_1)/S_1 \quad (2)$$

For a direct comparison of eCA activity, Chl *a*-specific activities are shown in Fig. 2a.

Activity of eCA in *P. tricornutum* was close to the detection limit ($S_1 \approx S_2 = S_3$; Figs. 1c and 2a), with slightly higher values only at the lowest CO₂ level (Figs. 1d and 2a). In *T. weissflogii*, eCA activity was significantly higher in all treatments (Figs. 1a,b and 2a). In cells acclimated to 36 ppmv CO₂, eCA activity was highest, but it decreased progressively with increasing pCO₂. Over the experimental CO₂ range, eCA activity varied by a factor of ~ 30 in this species (Fig. 2a).

In all CA measurements, injection of cells into the cuvette was followed by an immediate drop in log(enrichment) (Fig. 1). This drop is caused by diffusive entry of ¹³C¹⁸O¹⁸O into the cells, in which doubly labelled CO₂ is initially absent. In the presence of iCA, ¹⁸O loss from CO₂ of $m/z = 49$ is

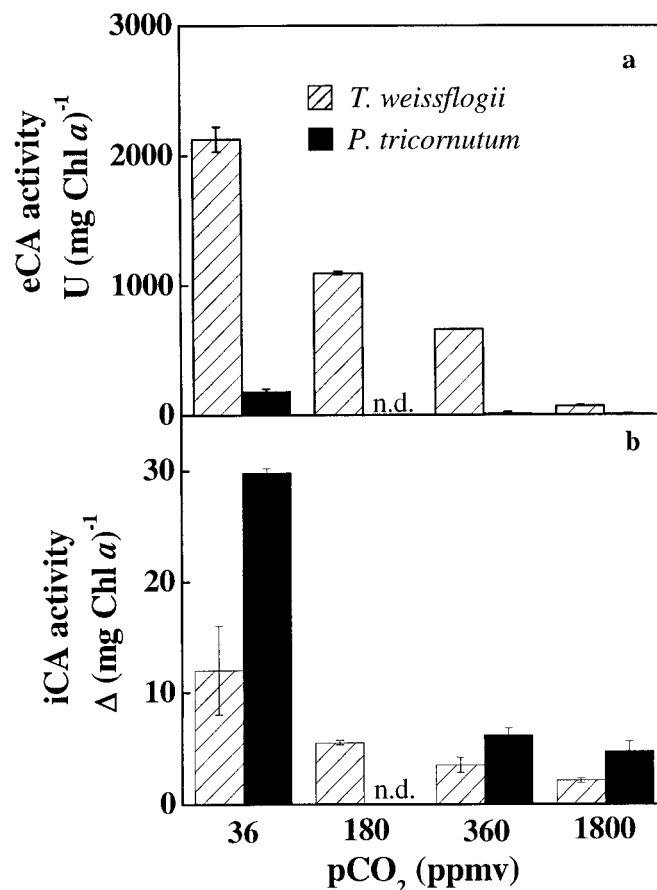


Fig. 2. Chl *a*-specific activities of (a) eCA and (b) iCA in *T. weissflogii* and *P. tricornutum* as a function of pCO₂ in the culture medium, to which the cells have been acclimated. n.d. = not determined.

catalyzed inside the cell, followed by diffusion of the newly generated CO₂ compounds ($m/z = 47$ and 45) back to the medium (Silverman 1982). In control experiments with cells from both species acclimated to 350 ppmv CO₂, the initial decline in log(enrichment) was almost 50% inhibited by 10 μM of the membrane permeable CA-inhibitor ethoxzolamide, whereas 200 μM were sufficient for almost complete suppression (data not shown). This indicates that internally localized CA(s) is (are) involved in the rapid exchange of doubly labeled CO₂ in both *P. tricornutum* and *T. weissflogii*. Both influx of $m/z 49$ and efflux of $m/z = 47$ and 45 add up to the initially observed rapid loss of ¹⁸O from the medium in the presence of cells. Subsequently, iCA-mediated ¹⁸O depletion from CO₂ in the medium solely depends on the balance between extracellular dehydration of ¹⁸O-containing HCO₃⁻ and the rate of CO₂ diffusion into the cell (Tu et al. 1986). In the absence of eCA activity, the resulting slope in our experiments approximated S_1 (Fig. 1).

As a measure of iCA activity, we followed the terminology of Palmqvist et al. (1994), who defined Δ as the drop in log(enrichment) when S_2 is extrapolated to the time of cell addition (Fig. 1). Because Δ is only determined by (1) the rate of diffusive CO₂ transport across cell membranes, (2)

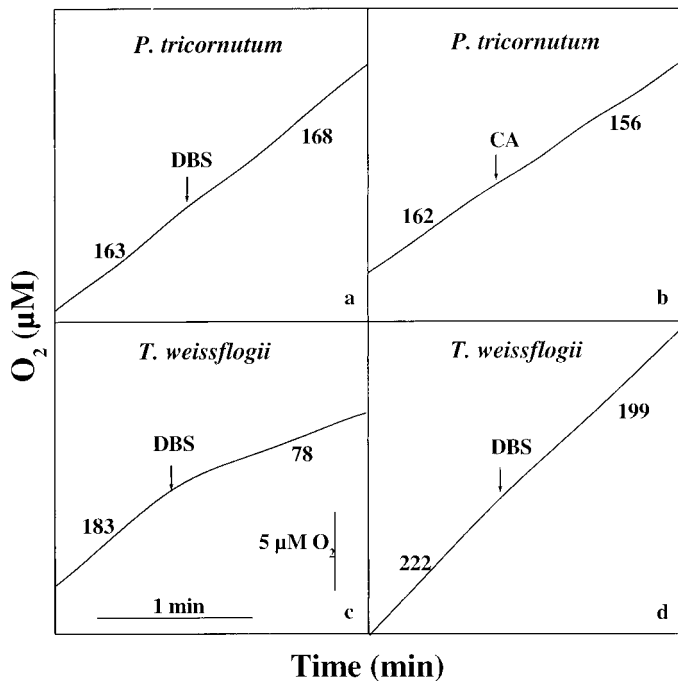


Fig. 3. Effect of the addition of the eCA-inhibitor DBS or commercially available CA on photosynthetic O₂ evolution in (a, b) *P. tricornutum* acclimated to 36 ppmv CO₂ and (c, d) *T. weissflogii* acclimated to 180 ppmv CO₂. The values close to the slopes indicate Chl *a*-specific rates [$\mu\text{mol} (\text{mg}^{-1} \text{Chl } a)^{-1} \text{h}^{-1}$] before and after addition of DBS/CA. Shown are typical experiments out of four to five independent replicates.

intracellular ¹⁸O depletion catalyzed by iCA, and (3) the rate of extracellular ¹⁸O depletion (spontaneous and eCA-catalyzed), correction for S₂ yields an estimate of iCA activity, expressed in arbitrary units. In contrast to measurements of eCA activity, determination of iCA activity is affected by the diffusive properties across cell membranes and the boundary layer surrounding the cells. Therefore, cell-specific characteristics such as intracellular pH, intracellular CO₂ concentrations, or cell size and shape potentially affect estimates of iCA activity, which prevents an interspecific comparison of enzymatic rates determined by this method. On the other hand, differences in these properties are less significant if one compares differently acclimated cells within each species.

Under the assumption that properties affecting CO₂ diffusion are similar for cells of a given species, Chl *a*-specific iCA estimates are directly comparable with each other. In analogy to eCA measurements, activity of iCA also depended on pCO₂ in the cultures. In both species we observed a significant decline in iCA activity with increasing pCO₂, reflected in an approximately sixfold change over the experimental CO₂ range (Fig. 2b). For a direct comparison of iCA activity between differently acclimated cells of each species, Chl *a*-specific activities are shown in Fig. 2b.

Inhibition of eCA activity by DBS had no effect on net photosynthesis in *P. tricornutum* grown at 36 ppmv CO₂ even at [CO_{2, aq}] = 1 μM in the assay medium (Fig. 3a),

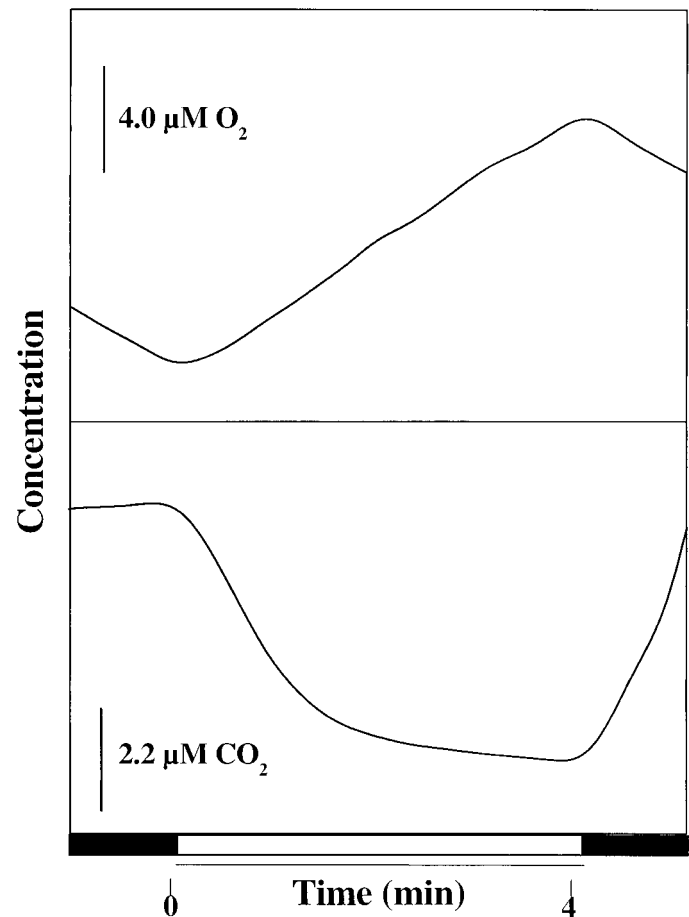


Fig. 4. Continuous measurements of O₂ and CO₂ concentrations used to estimate CO₂ uptake, HCO₃⁻ uptake, and photosynthetic O₂ evolution. Data shown in this figure were obtained with *T. weissflogii*, acclimated to 1,800 ppmv CO₂. The white bar at the bottom indicates a 4-min light period.

which represents the CO₂ concentration to which the culture was acclimated. Likewise, addition of CA had no effect on the photosynthetic rate (Fig. 3b). In *T. weissflogii* acclimated to 180 ppmv CO₂, inhibition of eCA caused a decline in net photosynthesis to less than half of the original value at [CO_{2, aq}] = 1 μM (Fig. 3c). When incubated at 13 μM of CO₂, the addition of DBS still affected photosynthesis, but the rate decreased by only ~10% (Fig. 3d).

CO₂ uptake, HCO₃⁻ uptake, and net photosynthesis—As indicated by a typical time course of changes in O₂ and CO₂ concentrations (Fig. 4), the transition from dark to light was accompanied by an immediate onset of photosynthetic O₂ production and CO₂ consumption. After ~3 min, the rate of decrease in CO₂ concentration in the cuvette reached steady state. When the light was turned off, photosynthetic O₂ production ceased immediately and was replaced by respiratory O₂ consumption. The initial CO₂ efflux in the dark caused the CO₂ concentration to increase rapidly.

Simultaneous uptake of CO₂ and HCO₃⁻ during steady-state photosynthesis was observed in both diatoms (Fig. 5,

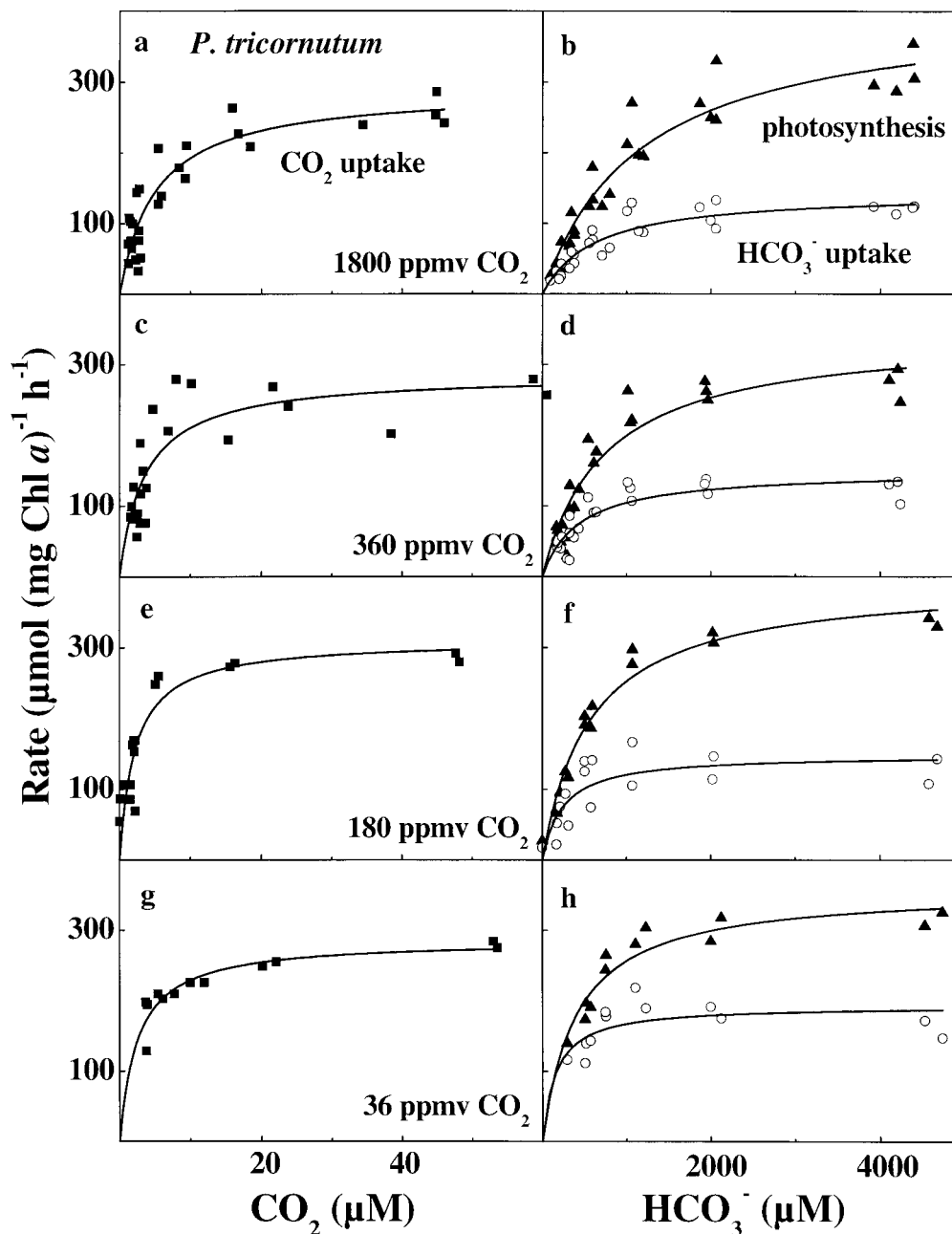


Fig. 5. *P. tricornutum*. Chl *a*-specific rates of gross CO₂ uptake (squares), HCO₃⁻ uptake (circles), and net photosynthesis (triangles) as a function of CO₂ or HCO₃⁻ concentration in the assay medium. Prior to the measurements, cultures were acclimated to (a, b) 1,800 ppmv; (c, d) 360 ppmv; (e, f) 180 ppmv; or (g, h) 36 ppmv of CO₂ for at least 48 h. Curves were obtained from a Michaelis-Menten fit.

6). However, species-specific substrate preferences for inorganic carbon uptake and differences in the effect of culture pCO₂ on uptake kinetics existed. Maximum rates (V_{\max}) and half-saturation concentrations ($K_{1/2}$) of inorganic carbon uptake and photosynthetic O₂ evolution were calculated from a Michaelis-Menten fit to the combined data of several independent measurements (Fig. 7).

In *P. tricornutum* maximum rates of gross CO₂ uptake,

HCO₃⁻ uptake, and net O₂ evolution were largely unaffected by acclimation to different pCO₂ (Figs. 5 and 7b). In general, rates of CO₂ uptake were approximately twice the rates of HCO₃⁻ uptake, which indicates that CO₂ was the preferred substrate for inorganic carbon uptake in this species. In *T. weissflogii*, maximum rates of HCO₃⁻ uptake and net O₂ evolution also remained largely unaffected by acclimation to a wide range of pCO₂ (Figs. 5 and 7a). A significant decrease

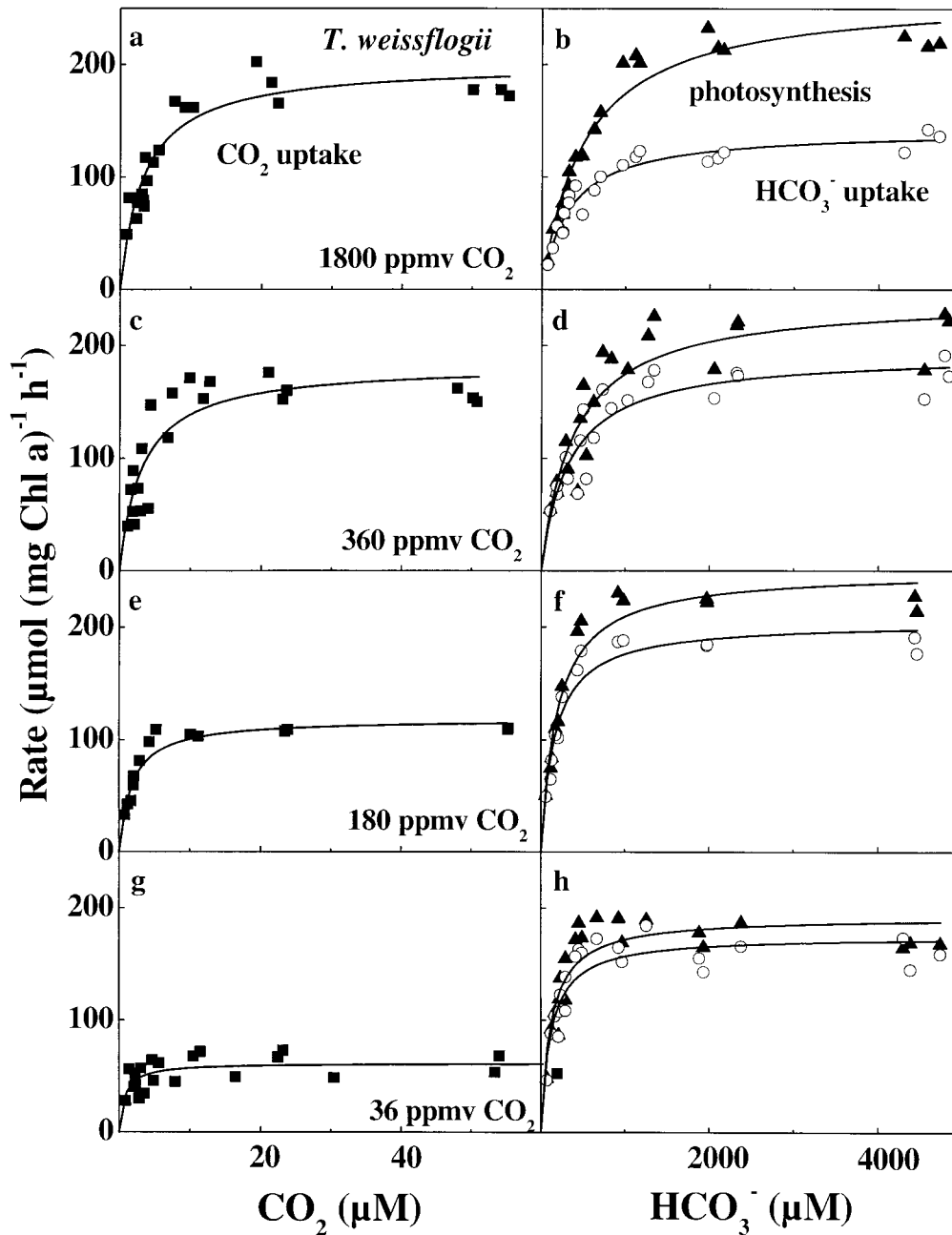


Fig. 6. *T. weissflogii*. Chl *a*-specific rates of gross CO₂ uptake (squares), HCO₃⁻ uptake (circles), and net photosynthesis (triangles) as a function of CO₂ or HCO₃⁻ concentration in the assay medium. Prior to the measurements, cultures were acclimated to (a, b) 1,800 ppmv; (c, d) 360 ppmv; (e, f) 180 ppmv; or (g, h) 36 ppmv of CO₂ for at least 48 h. Curves were obtained from a Michaelis-Menten fit.

in V_{\max} was only observed for HCO₃⁻ uptake at the highest pCO₂ and for photosynthetic O₂ evolution at the lowest pCO₂. Unlike *P. tricornutum*, however, V_{\max} of gross CO₂ uptake continuously decreased with decreasing pCO₂. This indicates that CO₂ was preferentially taken up by cells acclimated to 1,800 ppmv CO₂, whereas HCO₃⁻ uptake dominated in cells grown at 36 ppmv CO₂.

An increase in substrate affinities of carbon uptake upon

acclimation to decreasing CO₂ supply was observed in both diatoms, as was indicated by a decrease in $K_{1/2}(\text{CO}_2)$ of CO₂ uptake and in $K_{1/2}(\text{HCO}_3^-)$ of HCO₃⁻ uptake with decreasing pCO₂ in the cultures (Fig. 7c,d). Half-saturation of CO₂ uptake generally occurred at [CO_{2, aq}] ≤ 5 μM in both species. Half-saturation concentrations of HCO₃⁻ uptake were slightly lower in *T. weissflogii* than in *P. tricornutum* but were always <700 μM.

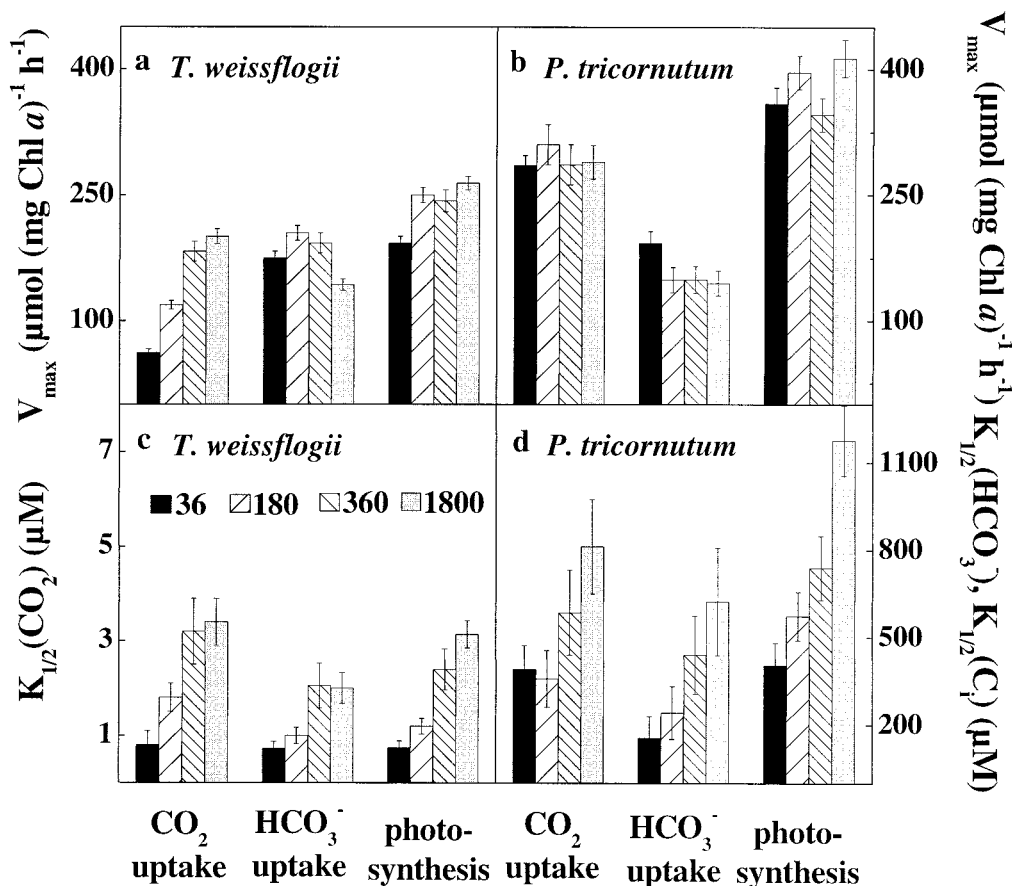


Fig. 7. V_{\max} and $K_{1/2}$ of gross CO_2 uptake, HCO_3^- uptake, and photosynthetic O_2 evolution for (b, d) *P. tricornutum* and (a, c) *T. weissflogii*. Kinetic parameters were calculated from a Michaelis-Menten fit to the combined data of several independent measurements. Error bars indicate ± 1 SD.

To evaluate the effect of a further decline in inorganic carbon availability on uptake kinetics, cultures of *P. tricornutum*, aerated with 36 ppmv CO_2 were harvested at a higher Chl *a* concentration ($250 \mu\text{g l}^{-1}$). In these cultures, the rate of CO_2 uptake exceeded the rate of CO_2 supply, so that CO_2

concentrations were no longer at equilibrium with the air stream. Consequently, $[\text{CO}_{2,\text{aq}}]$ dropped to $0.01 \mu\text{M}$, HCO_3^- decreased to $117 \mu\text{M}$, and pH increased to 10.1. Compared with experiments at 36 ppmv CO_2 under equilibrium conditions, V_{\max} of CO_2 and HCO_3^- uptake as well as $K_{1/2}(\text{CO}_2)$ of CO_2 uptake were largely unaffected by the further C_i depletion (Table 1). On the other hand, we observed a decline in $K_{1/2}(\text{HCO}_3^-)$ of HCO_3^- uptake by a factor of 10 under these conditions.

Similar kinetic constants were obtained in *P. tricornutum* cultivated at 36 ppmv CO_2 in the presence of buffer (20 mM HEPES) at a constant pH of 8.0 (Table 1). Equilibrium concentrations of CO_2 and HCO_3^- were 1.4 and $116 \mu\text{M}$ in the buffered cultures, but lower concentrations are, again, expected when cells are harvested at $250 \mu\text{g l}^{-1}$ Chl *a*. In both buffered and nonbuffered cultures, these extremely low concentrations of inorganic carbon yielded values of $K_{1/2}(\text{CO}_2) = 1.5\text{--}1.7 \mu\text{M}$ for CO_2 uptake and $K_{1/2}(\text{HCO}_3^-) = 12\text{--}15 \mu\text{M}$ for HCO_3^- uptake, regardless of a difference in pH by two units.

Discussion

Results from the present study indicate that small modifications of mass-spectrometric techniques, previously estab-

	CO_2 supply = CO_2 consumption, nonbuffered	CO_2 supply < CO_2 consumption	
		Nonbuffered	Buffered at pH 8.0
CO_2 uptake			
V_{\max}	285 (12)	282 (16)	256 (12)
$K_{1/2}(\text{CO}_2)$	2.4 (0.5)	1.7 (0.4)	1.5 (0.3)
HCO_3^- uptake			
V_{\max}	193 (14)	201 (10)	185 (9)
$K_{1/2}(\text{HCO}_3^-)$	155 (74)	12 (8)	15 (15)

lished to estimate inorganic carbon fluxes in cyanobacteria and freshwater microalgae (Badger et al. 1994; Palmqvist et al. 1994), provide the opportunity for such measurements in marine diatoms. This opens the field for the examination of organisms that constitute a large portion of marine primary production.

Several key aspects of inorganic carbon acquisition in the two diatoms tested here closely resemble general patterns previously observed in the freshwater chlorophytes *Chlamydomonas reinhardtii*, *Scenedesmus obliquus*, and the halotolerant *D. tertiolecta* (Badger et al. 1994; Palmqvist et al. 1994; Amoroso et al. 1998). These aspects include the capacity for simultaneous transport of CO₂ and HCO₃⁻ during photosynthesis even after growth at high CO₂ concentrations and the increase in the apparent affinities of both transport systems in response to diminishing supply of carbon substrate. Furthermore, iCA activity and, if present, eCA activity increased in response to a decrease in CO₂ concentration.

In spite of similarities in carbon acquisition among different taxa, we observed a number of species-specific characteristics. Most obvious is the high contribution of CO₂ uptake to total C_i uptake in *P. tricornutum* compared with the greater proportion of HCO₃⁻ uptake in *T. weissflogii*. Furthermore, the maximum rate of CO₂ uptake in *P. tricornutum* remains largely unaffected by variable pCO₂, whereas it decreases upon CO₂ depletion in *T. weissflogii*. Changes in V_{max} may indicate a change in the number of transport components in response to substrate availability. Another important difference between the species tested is the level of eCA activity. In fact, one reason for the choice of strain CCAP 1052/1A of *P. tricornutum* was the reported lack of eCA activity (John-McKay and Colman 1997), given that the absence of eCA activity is a prerequisite for C_i uptake measurements. In the absence of eCA, no inhibitor needs to be added during the assay.

Our results indicate that eCA activity of strain CCAP 1052/1A was close to the detection limit when cells were acclimated to pCO₂ levels of 360 ppmv or higher and remained low even in the lowest pCO₂ treatment. This finding is consistent with observations by John-McKay and Colman (1997) who—in a comparison of 11 strains of *P. tricornutum*—detected eCA activity in all but 3 strains of this species. Strain CCAP 1052/1A was among those three strains that lacked significant external CA activity. Because *P. tricornutum* showed a preference for CO₂ as the inorganic carbon source in our experiments, the low level of eCA expression in this organism is surprising. Interestingly, the addition of the eCA inhibitor DBS or addition of commercially available CA during measurements of photosynthetic rates both had no effect on net C_i fixation in this strain. This indicates that this strain of *P. tricornutum* has optimized its carbon uptake systems in a way that makes it largely independent of extracellular catalytic conversion of HCO₃⁻ to CO₂. In contrast, eCA activity appears to be crucial in other strains of *P. tricornutum*, as indicated by a significant decrease in photosynthetic CO₂ fixation by strain CCAP 1052/6 upon the addition of DBS in a study by Iglesias-Rodriguez and Merrett (1997). It should be noted here that the lack of response to the addition of DBS in our experiments with

strain CCAP 1052/1A demonstrates that the inhibitor itself has no effect on photosynthetic rates.

In *T. weissflogii*, where HCO₃⁻ appears to be the dominant C_i species taken up by the cells, especially at low CO₂ concentrations, one would expect that eCA activity plays a minor role in carbon acquisition. Nevertheless, this diatom expressed relatively high eCA activity, with a 30-fold increase in response to decreasing CO₂ availability. That eCA activity is beneficial for photosynthetic carbon fixation of *T. weissflogii* is supported by significantly higher photosynthetic rates in the absence of eCA inhibitor. In cells adapted to 180 ppmv CO₂, this effect was large at low [CO_{2,aq}] (1 μM) but small at higher [CO_{2,aq}] (13 μM). At 1 μM of CO₂, corresponding to ~90 μM of HCO₃⁻ at pH 8.0, cells acclimated to 180 ppmv CO₂ exhibited similar rates of CO₂ and HCO₃⁻ uptake. This indicates that, under limiting C_i concentrations, CO₂ supply is important for the cells.

Mass-spectrometric measurements of iCA activity have the advantage that highly reproducible results can be derived from living cells. For a given species, apparent activities are directly comparable after normalization for Chl *a* or cell numbers. Our in vivo estimates of iCA activity confirm the commonly accepted notion that the majority of microalgal species responds to CO₂ depletion with an increase in iCA activity. As in several other enzyme assays, a major drawback of this method is that the enzyme activity is in relative units, which cannot be directly converted into absolute rates (mol substrate catalyzed per unit of time). In addition, comparisons between species should be treated with caution, because measurements of internal CA activity that use the parameter Δ depend on the diffusive influx of doubly labeled CO₂ and thus on the diffusive properties of algal membranes. Therefore, it is reasonable to conclude that both species respond to a decrease in pCO₂ from 1,800 to 36 ppmv with an increase in iCA activity by a factor of six, which underlines the importance of iCA in inorganic carbon acquisition, although its function in eukaryotic microalgae is still not fully understood (Sültemeyer 1998). On the other hand, it is difficult to assess whether Δ values in *P. tricornutum* reflect higher iCA activity than in *T. weissflogii* or whether they are caused by more rapid diffusion of labelled CO₂ across the plasmalemma in the smaller species *P. tricornutum*.

Prior to the discussion of C_i flux estimates, we would like to summarize some of the assumptions underlying our calculations and how they potentially affect the results. A critical assessment of the method we used to estimate C_i fluxes is provided by Badger et al. (1994) and by Kaplan and Reinhold (1999). Critical assumptions that may affect C_i flux estimates concern the quantification of CO₂ efflux and the possibility of HCO₃⁻ efflux from the cells back to the medium. Quantification of CO₂ efflux assumes that the rate of diffusive CO₂ efflux in the light is well represented by the rate of CO₂ efflux during the first seconds of the subsequent dark phase. According to Badger et al. (1994), this method may underestimate actual rates of CO₂ efflux in eukaryotic microalgae as a result of cell compartmentation. Furthermore, we cannot exclude the possibility that an energy-driven transport of CO₂ out of the cell takes place in the light, leading to an underestimate of CO₂ efflux when it is determined from initial rates of CO₂ efflux during the first sec-

onds of the dark phase. In fact, massive CO₂ efflux originating from HCO₃⁻ uptake with subsequent intracellular conversion to CO₂ was proposed by Tchernov et al. (1997, 1998) on the basis of experiments with the cyanobacterium *Synechococcus* and with *Nannochloropsis* (Eustigmatophyceae). Any underestimate of CO₂ efflux would imply an underestimate of gross CO₂ uptake rates presented in this study.

Evidence for HCO₃⁻ efflux has, until now, only been reported for cyanobacteria (e.g., Salon et al. 1996; Kaplan and Reinhold 1999). Whether similar rates of HCO₃⁻ efflux can be achieved in eukaryotic microalgae, which accumulate intracellular C_i to a lesser degree and impose additional membrane barriers for HCO₃⁻ efflux, remains to be tested. Interpretation of HCO₃⁻ efflux is complicated by the use of inhibitors of photosynthetic carbon fixation, such as iodoacetamid, which are applied during these measurements. This approach has the advantage that HCO₃⁻ efflux can be measured while light energy is available for active transport processes. Because of the low permeability of biological membranes for HCO₃⁻, any HCO₃⁻ loss from a cell is likely to involve transport processes other than passive diffusion. On the other hand, evidence for HCO₃⁻ efflux during inhibition of C_i fixation still leaves the question whether this loss of inorganic carbon from the cell would also occur without impeding photosynthetic carbon fixation. No indication of HCO₃⁻ efflux was detected in *P. tricornutum* in the light (300 μmol photons m⁻² s⁻¹) when treated with 5 mM iodoacetamid (Sültemeyer unpubl. data).

If significant HCO₃⁻ efflux occurred in our assays, our estimates of HCO₃⁻ uptake would represent net uptake of HCO₃⁻. In other words, the method would still be capable of demonstrating the ability of direct HCO₃⁻ uptake accompanied by CO₂ uptake as an important additional carbon source in photosynthesis. However, $K_{1/2}(\text{HCO}_3^-)$ estimates obtained with this approach (Fig. 7) would be erroneous if large HCO₃⁻ efflux occurred. As long as we are unable to provide accurate measurements of HCO₃⁻ efflux during photosynthesis in the absence of inhibitors, the assumptions made in our calculations should be kept in mind when interpreting C_i uptake kinetics.

Our observation of simultaneous CO₂ and HCO₃⁻ uptake in marine diatoms is consistent with previous investigations (e.g., Colman and Rotatore 1995; Rotatore et al. 1995). In addition, results from the present study are the first individual estimates of CO₂ and HCO₃⁻ uptake rates during steady-state photosynthesis in marine diatoms that can be used to determine uptake kinetics for both uptake systems as a function of their respective substrates. Three main conclusions can be drawn from the high substrate affinities observed in the present study: (1) Even in cells acclimated to the highest pCO₂ level, half-saturation of CO₂ and HCO₃⁻ uptake was achieved at concentrations of 3.4–5.0 μM CO₂ and 325–623 μM HCO₃⁻. Compared with typical [CO_{2, aq}] of >10 μM and [HCO₃⁻] of ~2 mM in ocean surface waters, these results provide evidence for highly efficient CO₂ and HCO₃⁻ uptake in both diatoms. (2) As indicated by a continuous decrease in $K_{1/2}(\text{CO}_2)$ of CO₂ uptake and $K_{1/2}(\text{HCO}_3^-)$ of HCO₃⁻ uptake, both organisms were able to respond to diminishing carbon supply with a further increase in substrate affinity of their transport systems. (3) Similar to CO₂ uptake kinetics,

$K_{1/2}(\text{CO}_2)$ values of photosynthesis range from 1.3 to 5.8 μM CO₂, depending on species and culture conditions. In contrast, the few data available for kinetic properties of the CO₂-fixing enzyme Rubisco in diatoms are approximately one order of magnitude higher. According to Badger et al. (1998), half-saturation of the Rubisco carboxylase reaction is achieved at 31–36 μM in two strains of *Cylindrotheca* and at 41 μM in *P. tricornutum*. Higher CO₂ affinity of photosynthesis than of the Rubisco reaction provides evidence for the presence of a carbon-concentrating mechanism (CCM) that is maintained by active C_i transport.

Culture conditions in our experiments were chosen to simulate natural variations in surface ocean carbonate chemistry as closely as possible. Because any change in CO₂ concentration under natural conditions is accompanied by a change in pH, we purposely avoided adding buffer to the culture medium. Consequently, an increase from 36 to 1,800 ppmv CO₂ was accompanied by a decrease in pH from 9.1 to 7.6 and a decrease in the [HCO₃⁻]:[CO_{2, aq}] ratio from 767 to 32. As a result of the variable [HCO₃⁻]:[CO_{2, aq}] ratio, a 50-fold increase in [CO_{2, aq}] led to an increase in [HCO₃⁻] by only a factor of two. In this respect, buffered and nonbuffered seawater media differ considerably. Whereas both media aerated at different pCO₂ experience the same variation in [CO_{2, aq}] (1.4–70.5 μM in this study), the variation in [HCO₃⁻] is a lot less in buffered than in nonbuffered media (1.1–2.3 mM in this study, compared with 0.1–6.1 mM when buffered at pH 8.0).

The present study was not intended to evaluate the effect of buffer on C_i uptake kinetics. However, one experiment with *P. tricornutum*, in which extremely low CO₂ and HCO₃⁻ concentrations were achieved by photosynthetic C_i consumption (exceeding C_i supply), was performed with both buffered and nonbuffered culture medium. Results indicate that maximum substrate affinity of both CO₂ and HCO₃⁻ transport systems can be induced regardless of a difference in pH by two units (Table 1). In these experiments, $K_{1/2}(\text{CO}_2)$ of CO₂ uptake was only slightly lower than in nonbuffered cultures growing at equilibrium with 36 ppmv CO₂ in the air stream. In contrast, $K_{1/2}(\text{HCO}_3^-)$ of HCO₃⁻ uptake decreased drastically from 155 μM (at equilibrium with 36 ppmv CO₂, [HCO₃⁻] = 1,074 μM) to 12–15 μM (excess C_i consumption, [HCO₃⁻] < 117 μM HCO₃⁻). This indicates that the high-affinity HCO₃⁻ uptake system of *P. tricornutum* is not fully induced in nonbuffered cultures, even when they grow at equilibrium with 36 ppmv CO₂.

Evidence from studies of cyanobacteria suggests that CO₂ and HCO₃⁻ transport are separate, independent processes (Espie et al. 1991; Omata et al. 1999) and that HCO₃⁻ is involved as a primary signal to induce high-affinity HCO₃⁻ transport (Sültemeyer et al. 1998). Our results are consistent with these observations, although we cannot rule out the possibility that changes in CO₂ supply also affect HCO₃⁻ acquisition in the two diatoms of this study. If the CO₂ and HCO₃⁻ uptake systems operate independent of each other, this has important consequences for the interpretation of our results. As in any mass-spectrometric analysis, our measurements require constant pH in order to keep the rate constants of CO₂-HCO₃⁻ interconversion reactions invariable. Therefore, cells suspended in buffered assay medium experience,

in contrast to nonbuffered culture medium, constant $[\text{HCO}_3^-]:[\text{CO}_{2,\text{aq}}]$ ratios during flux measurements at any C_i concentration. Although this approach is appropriate to determine changes in CO_2 and HCO_3^- uptake capacities in relation to variable supply of the respective C_i species, calculated uptake kinetics are not truly representative of cells that have been acclimated in the absence of buffer.

To account for variable $[\text{HCO}_3^-]:[\text{CO}_{2,\text{aq}}]$ ratios during acclimation, we applied measured uptake kinetics (Fig. 7) to calculate CO_2 and HCO_3^- uptake rates as a function of the actual CO_2 and HCO_3^- concentrations to which the diatoms were exposed in the cultures. These calculations are based on the assumption that CO_2 and HCO_3^- transport systems are regulated independent of each other and that changes in pH have no significant effect on uptake kinetics. One important implication of such calculations is the effect on $\text{CO}_2:\text{HCO}_3^-$ uptake ratios at different culture conditions. In both species, we observe a systematic decrease in the $\text{CO}_2:\text{HCO}_3^-$ uptake ratio in response to a decrease in $p\text{CO}_2$ to which the cultures were acclimated (Fig. 8a). The horizontal line indicates the value at which CO_2 and HCO_3^- are taken up at equal proportions. It becomes evident that *P. tricornutum* prefers CO_2 as a substrate at all but the lowest $p\text{CO}_2$. In contrast, *T. weissflogii* shifts from CO_2 to HCO_3^- as preferred carbon substrate at $p\text{CO}_2 \leq 360$ ppmv. These results demonstrate that a decline in CO_2 supply is accompanied by the gradual induction of HCO_3^- uptake, whereas both species favor the uptake of CO_2 if present at high concentrations.

Such a regulatory mechanism raises the questions why marine diatoms, which have the capacity for active HCO_3^- transport, do not rely on the abundant HCO_3^- pool in seawater as the only inorganic carbon source. We suggest that the coexistence of both transport systems with preference for CO_2 uptake at higher CO_2 concentrations is maintained for energetic reasons. Even in the case of active CO_2 transport, its energetic cost is expected to be lower than that of HCO_3^- uptake, owing to the negative charge of this molecule and the inside-negative electric potential difference across the plasmalemma. Because marine phytoplankton evolved in an environment in which light supply is frequently limiting growth, the operation of a high-affinity CO_2 transport system may be advantageous from an energetic point of view.

Another way to minimize the substantial energetic costs associated with C_i uptake is to avoid inorganic carbon loss from the cell. Because we measured total C_i uptake and photosynthetic carbon fixation, mass balance calculations provide an estimate of inorganic carbon loss. The underlying assumptions are that carbon leakage from inside the cells back to the medium occurs mainly by diffusion of CO_2 and that the efflux of HCO_3^- is negligible. In this case, our calculations of C_i leakage (defined as the ratio of CO_2 efflux to total C_i uptake) indicate that $\sim 30\%$ of the inorganic carbon taken up is subsequently lost in both diatoms, when acclimated to $p\text{CO}_2 \leq 360$ ppmv (Fig. 8b). In response to a decrease in $p\text{CO}_2$ to 36 ppmv, leakage is minimized to values $< 10\%$. Such an increase in C_i assimilation efficiency may serve to reduce the higher energetic cost associated with an increased proportion of HCO_3^- taken up by low- CO_2 cells.

Our calculations of variable $\text{CO}_2:\text{HCO}_3^-$ uptake ratios

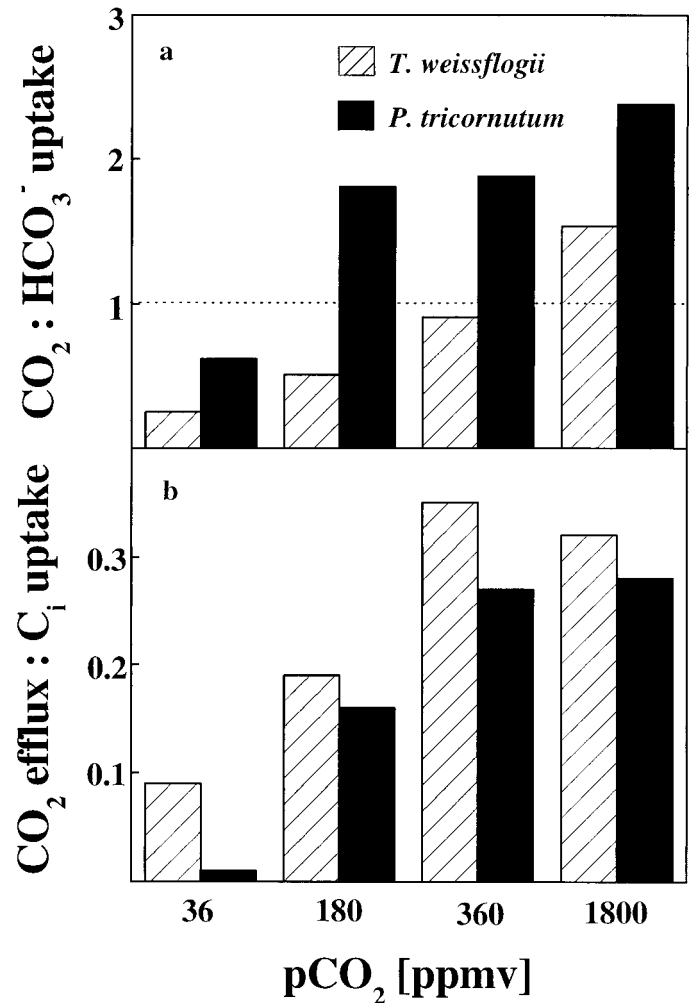


Fig. 8. Ratios of (a) gross $\text{CO}_2:\text{HCO}_3^-$ uptake and (b) CO_2 efflux: gross C_i uptake in *P. tricornutum* and *T. weissflogii* acclimated to different $p\text{CO}_2$. The dashed line indicates the value at which CO_2 and HCO_3^- are taken up at equal proportions.

and CO_2 leakage as a function of $p\text{CO}_2$ bear important implications for the interpretation of stable carbon isotope data. Several models of carbon isotope fractionation (ϵ_p) indicate that the key determinants are the isotopic composition $\delta^{13}\text{C}$ of the inorganic carbon source and the ratio of C_i influx to C_i efflux (Francois et al. 1993; Laws et al. 1995; Rau et al. 1996; Burkhardt et al. 1999). We applied the model of Burkhardt et al. (1999) to calculate isotope fractionation as a function of $[\text{CO}_{2,\text{aq}}]$ from our estimates of $\text{CO}_2:\text{HCO}_3^-$ uptake ratios and CO_2 leakage (Fig. 8) according to

$$\epsilon_p = a\epsilon_3 + \epsilon_2 F_{-1}/F_r \quad (3)$$

In this equation, a is the fractional contribution of HCO_3^- uptake to total C_i uptake F_r , F_{-1} is CO_2 efflux, ϵ_3 is the equilibrium fractionation between CO_2 and HCO_3^- (assumed to be -10%), and ϵ_2 is the enzymatic fractionation during carbon fixation (assumed to be 27%).

To evaluate whether our calculations of ϵ_p provide reasonable trends, we compared model results with ϵ_p values

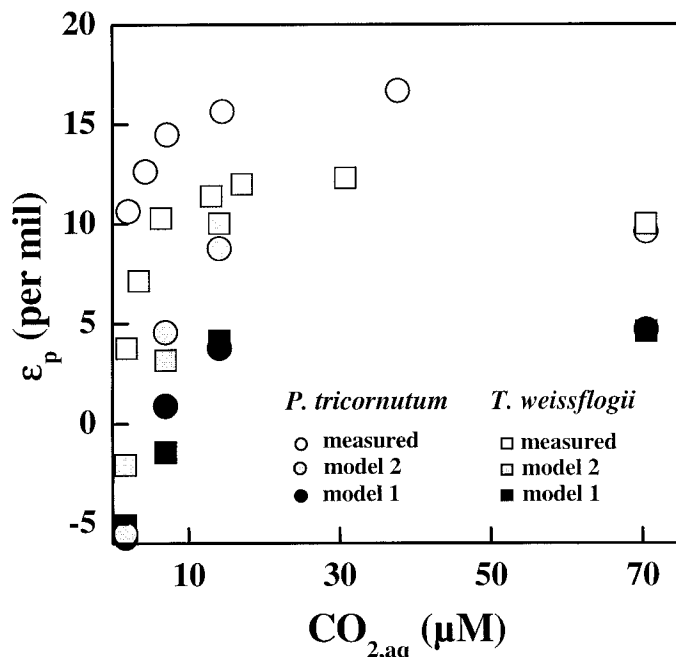


Fig. 9. Stable carbon isotope fractionation (ϵ_p) as a function of CO₂ concentration. Open symbols indicate measured data for *P. tricornutum* (Burkhardt et al. 1999) and *T. weissflogii* (U. Riebesell unpubl. data). Black symbols (model 1) represent ϵ_p values according to an isotope fractionation model (Burkhardt et al. 1999) that uses parameters obtained in this study. Gray symbols (model 2) indicate the effect of an increase in CO₂ efflux by a factor of two on ϵ_p . Further explanations are provided in the text.

measured in dilute batch cultures under nutrient-replete conditions in continuous light for *P. tricornutum*, strain CCAP1052/1A (Burkhardt et al. 1999) and *T. weissflogii* (U. Riebesell unpubl. data) (Fig. 9). As indicated by relatively constant fractionation at higher CO₂ concentrations and an increase in ϵ_p by ~9‰ over the experimental CO₂ range, our model calculations yield similar trends as direct measurements of ϵ_p . However, we observed a systematic offset by ~7‰ in *T. weissflogii* and by ~12‰ in *P. tricornutum* between measured and calculated ϵ_p . One should keep in mind that the isotope fractionation model can only serve as an approximation of ϵ_p because it neglects cell compartmentation, which is likely to have an impact on isotope fractionation (Burkhardt et al. 1999). Because the model is sensitive to photosynthetic rates, higher growth rates in the aerated cultures may also account for some of this discrepancy. Another important parameter in the calculation of ϵ_p is an accurate estimate of C_i fluxes. As discussed above, both an underestimate of CO₂ efflux and the neglect of HCO₃⁻ efflux may strongly influence flux estimates. In analogy to our calculation of C_i fluxes, HCO₃⁻ efflux is considered negligible in the isotope fractionation model. Therefore, it is difficult to assess how additional HCO₃⁻ efflux might affect ϵ_p . An increase in the relative contribution of HCO₃⁻ uptake to total uptake causes a decrease in ϵ_p that would make the discrepancy between calculated and measured fractionation even larger. On the other hand, higher ϵ_p values could the-

oretically be achieved if massive C_i efflux occurred at the same time. Much of the discrepancy between measurement and model calculations could also be explained in the absence of HCO₃⁻ efflux: higher rates of CO₂ efflux would lead to higher CO₂:HCO₃⁻ uptake ratios and to higher leakage values in Fig. 8. An increase in either parameter, in turn, would yield larger fractionation. As indicated in Fig. 9, an increase in CO₂ efflux by a factor of two would cause an increase in ϵ_p by ~5‰.

These considerations indicate that a systematic underestimate in CO₂ efflux may, in part, be responsible for the low ϵ_p values calculated by the fractionation model. Nevertheless, we were able to produce realistic trends in the ϵ_p versus [CO_{2,aq}] relationship on the basis of our C_i flux data, which provides evidence that the frequently observed decrease in ϵ_p in response to diminishing CO₂ supply may be the combined result of the gradual induction of HCO₃⁻ uptake and a decrease in CO₂ leakage.

In conclusion, results from this study indicate that, in spite of species-specific differences in certain aspects of C_i acquisition, the overall responses of the two marine diatoms tested here to changes in CO₂ supply closely resemble those reported for freshwater and halotolerant microalgae (Badger et al. 1994; Palmqvist et al. 1994; Amoroso et al. 1998). Highly efficient and inducible uptake mechanisms for both CO₂ and HCO₃⁻ demonstrate the capacity of these organisms to maintain high photosynthetic rates in response to large variations in the marine carbonate system. Even at CO₂ concentrations exceeding current levels in ocean surface waters by a factor of five, CO₂ uptake is supplemented by direct uptake of HCO₃⁻. On the other hand, our results clearly indicate that CO₂ remains an important substrate for photosynthesis even at CO₂ concentrations well below CO₂ levels typically encountered in the ocean. Under the assumption that CO₂ uptake requires less energy than HCO₃⁻ uptake, the advantage of a highly efficient CO₂ uptake mechanism may be to facilitate photosynthetic performance in a light-limited environment.

References

- AMOROSO, G., D. SÜLTEMEYER, C. THYSSEN, AND H. P. FOCK. 1998. Uptake of HCO₃⁻ and CO₂ in cells and chloroplasts from the microalgae *Chlamydomonas reinhardtii* and *Dunaliella tertiolecta*. *Plant Physiol.* **116**: 193–201.
- BADGER, M. R., T. J. ANDREWS, S. M. WHITNEY, M. LUDWIG, D. C. YELLOWLEES, W. LEGGAT, AND G. D. PRICE. 1998. The diversity and coevolution of Rubisco, plastids, pyrenoids, and chloroplast-based CO₂-concentrating mechanisms in algae. *Can. J. Bot.* **76**: 1052–1071.
- , K. PALMQVIST, AND J.-W. YU. 1994. Measurement of CO₂ and HCO₃⁻ fluxes in cyanobacteria and microalgae during steady-state photosynthesis. *Physiol. Plant.* **90**: 529–536.
- , AND G. D. PRICE. 1989. Carbonic anhydrase activity associated with the cyanobacterium *Synechococcus* PCC7942. *Plant Physiol.* **89**: 51–60.
- BURKHARDT, S., U. RIEBESELL, AND I. ZONDERVAN. 1999. Effects of growth rate, CO₂ concentration, and cell size on the stable carbon isotope fractionation in marine phytoplankton. *Geochim. Cosmochim. Acta* **63**: 3729–3741.

- BURNS, B. D., AND J. BEARDALL. 1987. Utilization of inorganic carbon by marine microalgae. *J. Exp. Mar. Biol. Ecol.* **107**: 75–86.
- COLMAN, B., AND C. ROTATORE. 1995. Photosynthetic inorganic carbon uptake and accumulation in two marine diatoms. *Plant Cell Environment* **18**: 919–924.
- ELZENGA, J. T., H. B. A. PRINS, AND J. STEFELS. 2000. The role of extracellular carbonic anhydrase activity in inorganic carbon utilization of *Phaeocystis globosa* (Prymnesiophyceae): A comparison with other marine algae using the isotopic disequilibrium technique. *Limnol. Oceanogr.* **45**: 372–380.
- ESPIE, G. S., A. G. MILLER, AND D. T. CANVIN. 1991. High affinity transport of CO₂ in the cyanobacterium *Synechococcus* UTEX 625. *Plant Physiol.* **97**: 943–953.
- FRANCOIS, R., M. A. ALTABET, AND R. GOERICKE. 1993. Changes in the δ¹³C of surface water particulate organic matter across the subtropical convergence in the SW Indian Ocean. *Global Biogeochem. Cycles* **7**: 627–644.
- GOYET, C., AND A. POISSON. 1989. New determination of acid dissociation constants in seawater as a function of temperature and salinity. *Deep-Sea Res.* **36**: 1635–1654.
- GUILLARD, R. R. L., AND J. H. RYTHER. 1962. Studies of marine planktonic diatoms. *Can. J. Microbiol.* **8**: 229–239.
- HOUGHTON, J. T., L. G. MEIRA FILHO, B. A. CALLANDER, N. HARRIS, A. KATTENBERG, AND K. MASKELL [EDS.]. 1996. Climate change 1995. The science of climate change—contribution of WGI to the second assessment report of the Intergovernmental Panel of Climate Change. Cambridge Univ. Press.
- IGLESIAS-RODRIGUEZ, M. D., AND M. J. MERRETT. 1997. Dissolved inorganic carbon utilization and the development of extracellular carbonic anhydrase by the marine diatom *Phaeodactylum tricorutum*. *New Phytol.* **135**: 163–168.
- JOHNSON, K. M., K. D. WILLS, D. B. BUTLER, W. K. JOHNSON, AND C. S. WONG. 1993. Coulometric total carbon dioxide analysis for marine studies: Maximizing the performance of an automated gas extraction system and coulometric detector. *Mar. Chem.* **44**: 167–187.
- JOHN-MCKAY, M. E., AND B. COLMAN. 1997. Variation in the occurrence of external carbonic anhydrase among strains of the marine diatom *Phaeodactylum tricorutum* (Bacillariophyceae). *J. Phycol.* **33**: 988–990.
- KAPLAN, A., AND L. REINHOLD. 1999. CO₂ concentrating mechanisms in photosynthetic microorganisms. *Annu. Rev. Plant Physiol. Plant Mol. Biol.* **50**: 539–570.
- , AND OTHERS. 1998. The inorganic carbon-concentrating mechanism in cyanobacteria: induction and ecological significance. *Can. J. Bot.* **76**: 917–924.
- KORB, R. E., P. J. SAVILLE, A. M. JOHNSTON, AND J. A. RAVEN. 1997. Sources of inorganic carbon for photosynthesis by three species of marine diatom. *J. Phycol.* **33**: 433–440.
- LAW, E. A., B. N. POPP, R. R. BIDIGARE, M. C. KENNICUTT, AND S. A. MACKO. 1995. Dependence of phytoplankton carbon isotopic composition on growth rate and [CO₂]_{aq}: Theoretical considerations and experimental results. *Geochim. Cosmochim. Acta* **59**: 1131–1138.
- LI Q., AND D. T. CANVIN. 1998. Energy sources for HCO₃⁻ and CO₂ transport in air-grown cells of *Synechococcus* UTEX 625. *Plant Physiol.* **116**: 1125–1132.
- MILLER, A. G., G. S. ESPIE, AND D. T. CANVIN. 1991. Active CO₂ transport in cyanobacteria. *Can. J. Bot.* **69**: 925–935.
- NIMER, N. A., M. D. IGLESIAS-RODRIGUEZ, AND M. J. MERRETT. 1997. Bicarbonate utilization by marine phytoplankton species. *J. Phycol.* **33**: 625–631.
- OMATA, T., G. D. PRICE, M. R. BADGER, M. OKAMURA, S. GOHTA, AND T. OGAWA. 1999. Identification of an ATP-binding cassette transporter involved in bicarbonate uptake in the cyanobacterium *Synechococcus* sp. Strain PCC 7942. *Proc. Natl. Acad. Sci.* **96**: 13571–13576.
- PALMQVIST, K., Z. RAMAZANOV, AND G. SAMUELSSON. 1990. The role of extracellular carbonic anhydrase for accumulation of inorganic carbon in the green alga *Chlamydomonas reinhardtii*. A comparison between wild-type and cell-wall-less mutant cells. *Physiol. Plant.* **80**: 267–276.
- , J.-W. YU, AND M. R. BADGER. 1994. Carbonic anhydrase activity and inorganic carbon fluxes in low- and high-C_i cells of *Chlamydomonas reinhardtii* and *Scenedesmus obliquus*. *Physiol. Plant.* **90**: 537–547.
- RAU, G. H., U. RIEBESELL, AND D. WOLF-GLADROW. 1996. A model of photosynthetic ¹³C fractionation by marine phytoplankton based on diffusive molecular CO₂ uptake. *Mar. Ecol. Prog. Ser.* **133**: 275–285.
- RAVEN, J. A. 1997. Inorganic carbon acquisition by marine autotrophs. *Adv. Bot. Res.* **27**: 85–209.
- . 1980. Nutrient transport in microalgae. *Adv. Microb. Physiol.* **21**: 47–226.
- ROTATORE, C., AND B. COLMAN. 1991. The localization of active inorganic carbon transport at the plasma membrane in *Chlorella ellipsoidea*. *Can. J. Bot.* **69**: 1025–1031.
- , AND ———. 1992. Active uptake of CO₂ by the diatom *Navicula pelliculosa*. *J. Exp. Bot.* **43**: 571–576.
- , ———, AND M. KUZMA. 1995. The active uptake of carbon dioxide by the marine diatoms *Phaeodactylum tricorutum* and *Cyclotella* sp. 1995. *Plant Cell Environment* **18**: 913–918.
- , R. R. LEW, AND B. COLMAN. 1992. Active uptake of CO₂ during photosynthesis in the green alga *Eremosphaera viridis* is mediated by a CO₂-ATPase. *Planta* **188**: 539–545.
- SALON, C., N. A. MIR, AND D. T. CANVIN. 1996. HCO₃⁻ and CO₂ leakage from *Synechococcus* UTEX 625. *Plant Cell Environment* **19**: 260–274.
- SILVERMAN, D. N. 1982. Carbonic anhydrase. Oxygen-18 exchange catalyzed by an enzyme with rate-contributing proton-transfer steps. *Methods Enzymol.* **87**: 732–752.
- SÜLTEMAYER, D. 1998. Carbonic anhydrase in eukaryotic algae: Characterization, regulation, and possible function during photosynthesis. *Can. J. Bot.* **76**: 962–972.
- , H. P. FOCK, AND D. T. CANVIN. 1990. Mass spectrometric measurement of intracellular carbonic anhydrase activity in high and low C_i cells of *Chlamydomonas*. *Plant Physiol.* **94**: 1250–1257.
- , B. KLUGHAMMER, M. R. BADGER, AND G. D. PRICE. 1998. Fast induction of high-affinity HCO₃⁻ transport in cyanobacteria. *Plant Physiol.* **116**: 183–192.
- , G. D. PRICE, J.-W. YU, AND M. R. BADGER. 1995. Characterization of carbon dioxide and bicarbonate transport during steady-state photosynthesis in the marine cyanobacterium *Synechococcus* strain PCC7002. *Planta* **197**: 597–607.
- TCHERNOV, D., M. HASSIDIM, A. VARDI, B. LUZ, A. SUKENIK, L. REINHOLD, AND A. KAPLAN. 1998. Photosynthesizing marine microorganisms can constitute a source of CO₂ rather than a sink. *Can. J. Bot.* **76**: 949–953.
- , ———, B. LUZ, A. SUKENIK, L. REINHOLD, AND A. KAP-

- LAN. 1997. Sustained net CO₂ evolution during photosynthesis by marine microorganisms. *Current Biol.* **7**: 723–728.
- TORTELL, P. D., J. R. REINFELDER, AND F. M. M. MOREL. 1997. Active bicarbonate uptake by diatoms. *Nature* **390**: 243–244.
- TU, C. K., M. AVECEDO-DUNCAN, C. G. WYNNS, AND D. N. SILVERMAN. 1986. Oxygen-18 exchange as a measure of the accessibility of CO₂ and HCO₃⁻ to carbonic anhydrase in *Chlorella vulgaris* (UTEX 263). *Plant Physiol.* **85**: 72–77.

Received: 2 November 2000

Accepted: 12 April 2001

Amended: 18 May 2001